Exploring the Nuclear Phase Diagram with Beam Energy Scans

Stephen Horvat

E-mail: stephen.horvat@yale.edu

Abstract. The nuclear phase diagram is mapped using beam energy scans of relativistic heavy-ion collisions. This mapping is possible because different collision energies develop along different trajectories through the phase diagram. High energy collisions will evolve though a crossover phase transition according to lattice QCD, but lower collision energies may traverse a first order phase transition. There are hints for this first order phase transition and its critical endpoint, but further measurements and theoretical guidance is needed. In addition to mapping the phase transition, beam energy scans allow us to see if we can turn off the signatures of deconfinement. If an observable is a real signature for the formation of the deconfined state called quark-gluon plasma, then it should turn off at sufficiently low collision energies. In this summary talk I will show the current state of the field using beam energy scan results from RHIC and SPS, I will show where precise theoretical guidance is needed for understanding recent measurements, and I will motivate the need for more data and new measurements from FAIR, NICA, RHIC, and the SPS.

1. Introduction

When the SPS began operations it reached collision energies where many theorists expected the onset of deconfinement [1]. Early observables for deconfinement were compelling, but many in the field thought that they could also be explained by other phenomena. Taking the "horn" in K^+/π^+ produced in heavy-ion collisions as a function of $\sqrt{s_{\rm NN}}$ as an example, several models that did not include a deconfined partonic phase were able to explain the data [2]. It was not until RHIC observed jet energy-loss signatures at higher energies as well as strong azimuthal anisotropy in particle distributions that the majority of the heavy-ion community became convinced that a strongly interacting QGP phase had been produced [3, 4, 5, 6]. The SPS, RHIC, and the LHC have gone on to provide many additional measurements that constrain the properties of, and the evolution of, the produced medium.

Central collisions at the LHC and at the highest RHIC energies form regions with very high initial energy and entropy densities. These overlap regions evolve hydrodynamically to follow different trajectories through the QCD phase diagram depending on their initial conditions [7, 8], where lower energy collisions follow a trajectory with a higher baryon chemical potential [9]. While lattice simulations of the QCD equation of state predict a crossover phase transition from a hadronic gas to partonic degrees of freedom for small values of baryon chemical potential as the temperature is increased above a critical value, at higher values of the baryon chemical potential their may be a first order phase transition [10]. One of the purposes of beam energy scans (BESs) in heavy ion collisions is to identify the order of the phase transition and locate its corresponding critical point if it exists. The other purpose is to test that signatures of

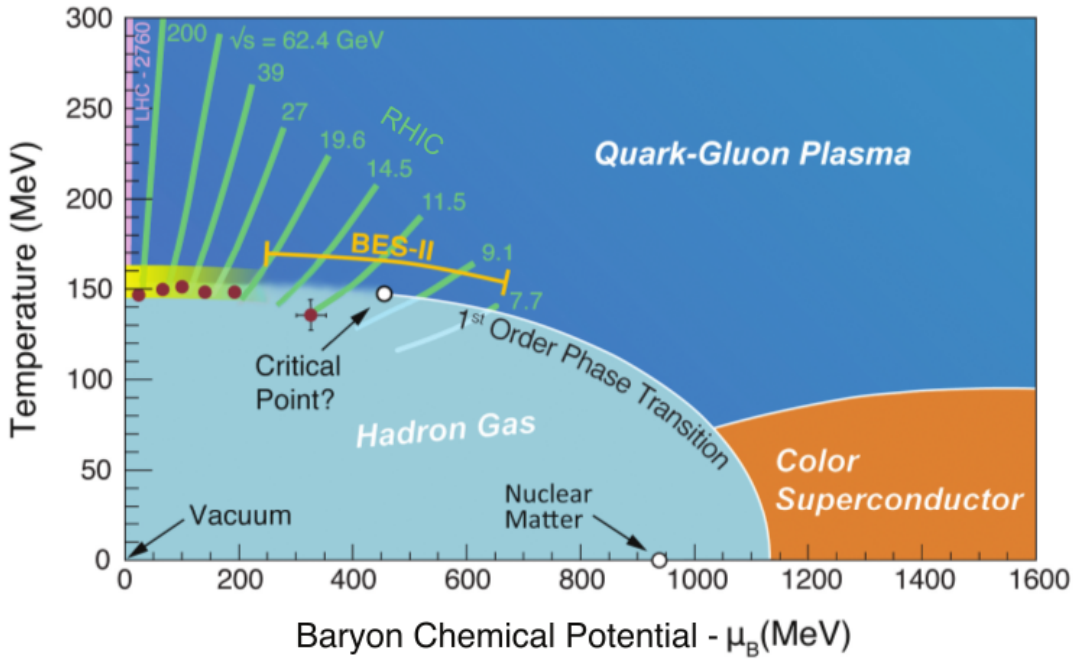

Figure 1. A cartoon of the QCD phase diagram [7].

deconfinement 'turn off' as the collision energy is decreased and to constrain the conditions required to form QGP.

2. Turning off signatures of QGP formation

There are many proposed signatures for the formation of QGP, but they generally fall into three classes: probes produced early in the collision that go on to interact with the medium, radiation from the medium, and final state particles that are formed from constituents of the medium. For the first class we consider as early probes high transverse momentum (p_{T}) partons that interact strongly with QGP losing energy in a process called jet-quenching.

The nuclear modification factor, R_{AA}, is the number of particles measured at a particular p_{T} in a heavy ion collision divided by what we would expect from independent nucleonic scatterings. To model these independent nucleonic scatterings we estimate how many of them there were by using a Glauber Monte Carlo [12] and then scale the number of particles measured at the same p_{T} in proton-proton collisions up by this number. If $R_{\mathrm{AA}} = 1$ then either there are no modifications from colliding heavy nuclei relative to colliding protons, or there is a balancing of enhancement and suppression effects. However, if $R_{\mathrm{AA}} \ll 1$ at high-p_{T} then this may be explained by high momentum particles losing momentum in QGP. Figure 2 shows R_{AA} for several collision energies from the SPS, RHIC, and the LHC [11]. While RHIC and the LHC measured large suppression at high-p_{T}, the SPS found $R_{\mathrm{AA}} = 1$ for pions at mid-rapidity. Here we want to separate the idea of turning off QGP formation from the idea of turning off a signature for QGP formation. Depending on the measurement's sensitivity to QGP the signature may ''turn off' even though QGP is still being formed. The relative time spent in a partonic phase as well as the spacial extent of the partonic phase at hadronization can be expected to be reduced as collision energies are reduced. The best signatures for QGP formation will be those that are maximally sensitive to the partonic phase and minimally effected by other phenomena. In the case of R_{AA}, measurements of strong enhancement at $\sqrt{s_{\mathrm{NN}}} = 7.7$ GeV demonstrate that

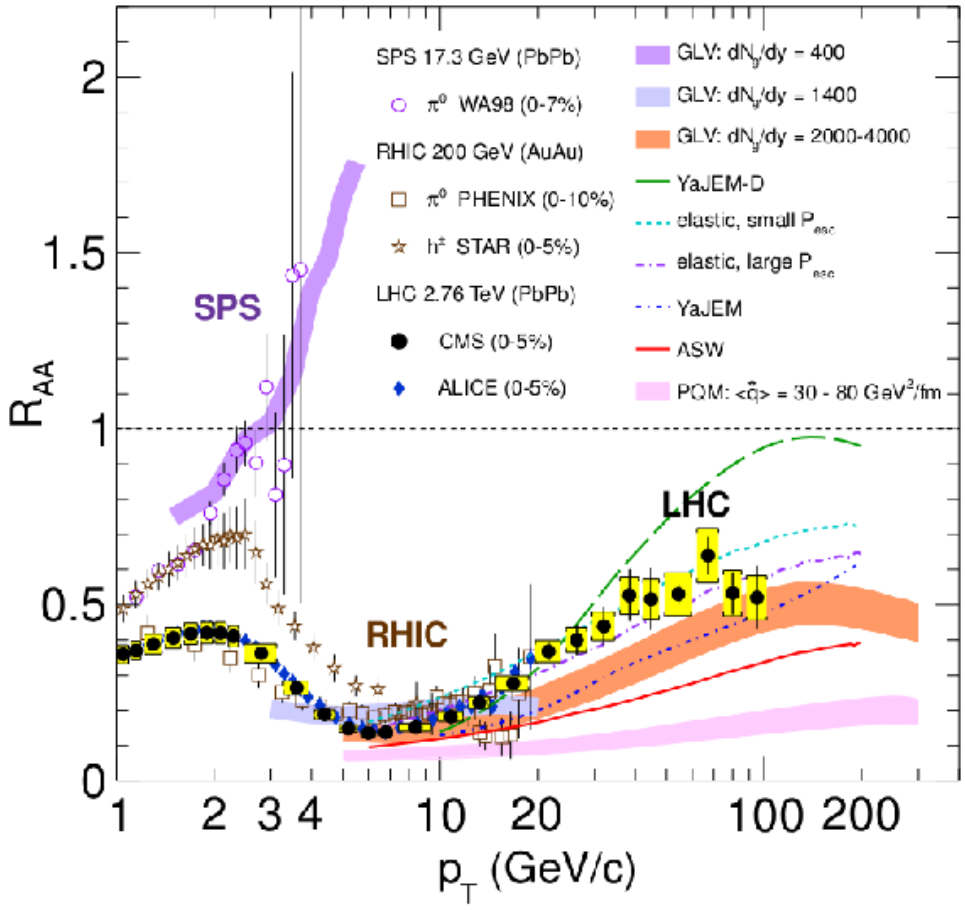

Figure 2. World data for $R_{\rm AA}$ [11].

$R_{\rm AA}$ is strongly effected by enhancement phenomena that make this observable less sensitive to QGP formation at SPS and RHIC BES energies [13]. Alternative observables for high-$p_{\rm T}$ probes suggest deconfinement may persist at least down to $\sqrt{s_{\rm NN}} = 14.5$ GeV [13, 14].

3. First Order Phase Transition

While the previous signatures give information about what phases the medium evolves through, it is also interesting to determine the nature of the phase transition. While lattice calculations tell us that the transition at small baryon chemical potential (μ_B) is a crossover, there have been suggestions that there may be a first or second order phase transition at higher μ_B [15, 16, 17, 18, 19]. It has been shown that the pressure and speed of sound in the medium would have minima near a first order phase transition and that this would lead to a characteristic shape in the directed flow measured in heavy-ion collisions [20, 21, 22, 23]. Measurements from STAR are shown in Fig. 3 where we see trends that are consistent with the predicted trends [24].

PHENIX accessed the same underlying physical processes using a different observable with Hanbury Brown and Twist (HBT) data that were collected by ALICE, PHENIX, and STAR [25]. Here the $(\mathrm{R_{out}})^2 - (\mathrm{R_{side}})^2$ in Fig. 4(a) is related to emission duration while the quantity in Fig. 4(b) is related to the speed of sound [24, 26].

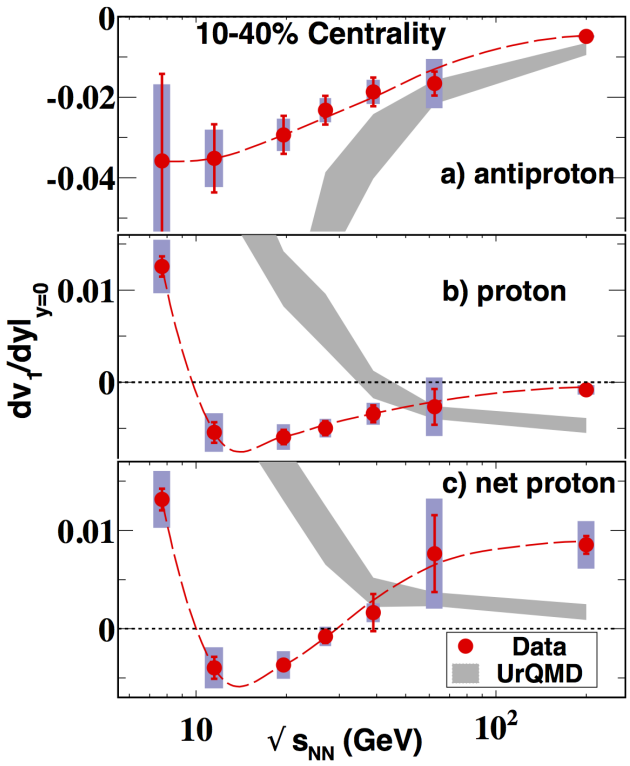

Figure 3. The slope of v_1 versus rapidity as a function of $sqrts_{\rm NN}$ for mid-central (10-40%) collisions for antiprotons (a), protons (b), and net protons (c), and compared to UrQMD [24].

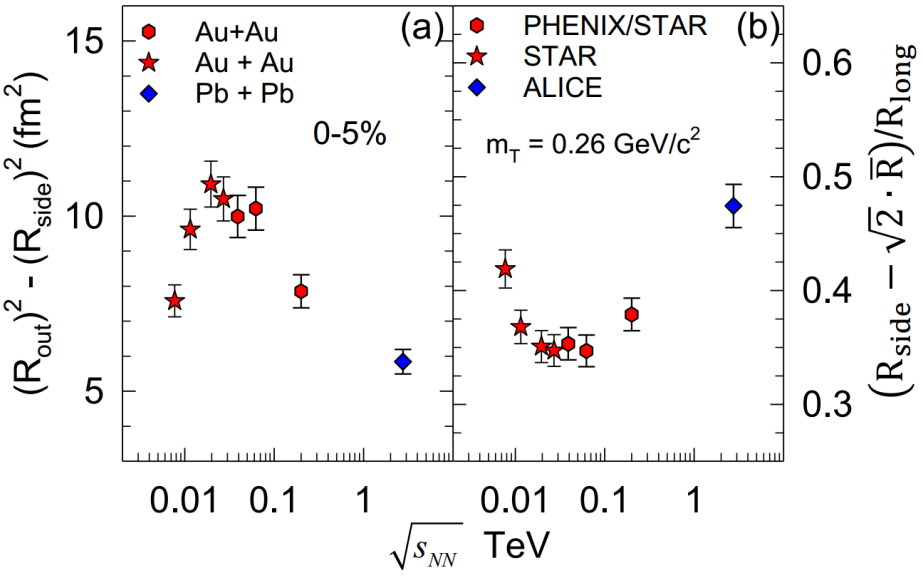

Figure 4. Two non-monotonic arangements of HBT data are shown for 0-5% centrality. The left panel is related to emmision duration and has a maximum in the range of $\sqrt{s_{\rm NN}}$ = 19.6 - 39 GeV. The right panel is related to the speed of sound and has a minimum in the range of $\sqrt{s_{\rm NN}}$ = 19.6 - 62.4 GeV [25].

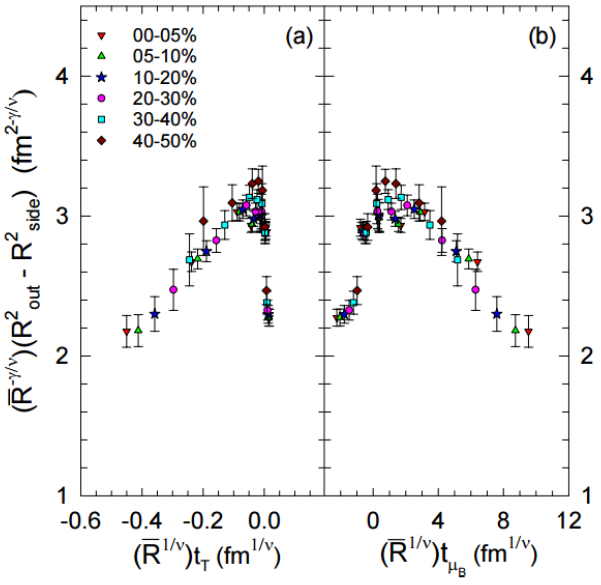

Figure 5. Finite scaling of HBT data using critical exponents collapses the data for multiple energies and centralities onto a single curve with the critical point estimated at $T^{cep} \approx 165$ MeV and $\mu_B^{cep} \approx 95$ MeV [26].

4. Critical End Point

Near a critical point there would be a divergence of susceptibilities and conserved quantities would have increased fluctuations [27]. PHENIX and STAR have measured the energy dependence of higher moments of net charge [28, 29]. While these results did not locate the critical point, more data and larger acceptance will be available for RHIC BES II.

Figure 5 shows a measurement that does suggest both the existence and the location of the critical point by doing a finite size scaling of HBT data using critical exponents [26]. This analysis found critical exponents $\nu \approx 0.66$ and $\gamma \approx 1.2$ and the location of the critical point to be $T^{cep} \approx 165$ MeV and $\mu_B^{cep} \approx 95$ MeV. The idea here is that with the proper description of the data, the data will all point toward the critical point even if the trajectories of individual collisions, such as those at the LHC, do not pass particularly close to the critical point. This is similar to the method that was used earlier to determine the location of the liquid-vapor critical point [30]. This work was carried further by showing that these same critical exponents can be used to scale the moments of net proton distributions [31].

5. Summary

With a couple of possible exceptions [26, 31] these signatures do not characterize the order of the phase transition or describe the location of a critical point but with more observables, data, and detector upgrades the SPS, RHIC, FAIR and NICA are poised to gather the data over a broad range of energies and collision systems. In order to coordinate the work of theorists who are working to describe in quantitative detail the different stages of evolution in heavy-ion collisions at low energies, and to provide direction to experimentalists, a new theory collaboration has been formed called the Beam Energy Scan Theory (BEST) collaboration. The next few years will see BES data being collected at four different experimental facilities and the coordination of BES theorists in order to map the QCD phase diagram.

References

[1] K. Kajantie. Quark Matter '84, Helsinki, 17–21 June 1984. *Nucl. Phys.*, A956:907–910, 2016.

[2] Jajati K. Nayak, S. Banik, and Jan-e Alam. The horn in the kaon to pion ratio. *Phys. Rev.*, C82:024914, 2010.

[3] I. Arsene et al. *Nucl.Phys.*, A **757**:1–27, 2005.

[4] B.B. Back et al. *Nucl.Phys.*, A **757**:28–101, 2005.

[5] John Adams et al. *Nucl.Phys.*, A **757**:102–183, 2005.

[6] K. Adcox et al. *Nucl.Phys.*, A **757**:184–283, 2005.

[7] Ani Aprahamian et al. Reaching for the horizon: The 2015 long range plan for nuclear science. 2015.

[8] Chiho Nonaka and Masayuki Asakawa. Hydrodynamical evolution near the QCD critical end point. *Phys. Rev.*, C71:044904, 2005.

[9] J. Cleymans, H. Oeschler, K. Redlich, and S. Wheaton. Status of chemical freeze-out. *J. Phys.*, G32:S165–S170, 2006.

[10] Z. Fodor and S. D. Katz. Critical point of QCD at finite T and mu, lattice results for physical quark masses. *JHEP*, 04:050, 2004.

[11] Serguei Chatrchyan et al. Study of high-pT charged particle suppression in PbPb compared to *pp* collisions at $\sqrt{s_{NN}} = 2.76$ TeV. *Eur. Phys. J.*, C72:1945, 2012.

[12] Michael L. Miller, Klaus Reygers, Stephen J. Sanders, and Peter Steinberg. *Ann.Rev.Nucl.Part.Sci.*, **57**:205–243, 2007.

[13] Stephen P. Horvat. Measurement of hadron suppression and study of its connection with vanishing v_3 at low $\sqrt{s_{\rm NN}}$ in Au+Au collisions with STAR. *Nucl. Phys.*, A956:838–841, 2016.

[14] James D. Brandenburg. Identified Light and Strange Hadron Spectra at $\sqrt{s_{NN}}$=14.5 GeV and Systematic Study of Baryon/Meson Effect at Intermediate Transverse Momentum with STAR at RHIC BES I. *Nucl. Phys.*, A956:445–448, 2016.

[15] Juergen Berges and Krishna Rajagopal. Color superconductivity and chiral symmetry restoration at nonzero baryon density and temperature. *Nucl. Phys.*, B538:215–232, 1999.

[16] Yoshitaka Hatta and Takashi Ikeda. Universality, the QCD critical / tricritical point and the quark number susceptibility. *Phys. Rev.*, D67:014028, 2003.

[17] Mikhail A. Stephanov. QCD phase diagram and the critical point. *Prog. Theor. Phys. Suppl.*, 153:139–156, 2004. [Int. J. Mod. Phys.A20,4387(2005)].

[18] Masayuki Asakawa and Chiho Nonaka. Critical end point and its consequences. *Nucl. Phys.*, A774:753–756, 2006.

[19] Philippe de Forcrand, Jens Langelage, Owe Philipsen, and Wolfgang Unger. Lattice QCD Phase Diagram In and Away from the Strong Coupling Limit. *Phys. Rev. Lett.*, 113(15):152002, 2014.

[20] Dirk H. Rischke, Yaris Pursun, Joachim A. Maruhn, Horst Stoecker, and Walter Greiner. The Phase transition to the quark - gluon plasma and its effects on hydrodynamic flow. *Heavy Ion Phys.*, 1:309–322, 1995.

[21] L. P. Csernai and D. Rohrich. Third flow component as QGP signal. *Phys. Lett.*, B458:454, 1999.

[22] J. Brachmann, S. Soff, A. Dumitru, Horst Stoecker, J. A. Maruhn, W. Greiner, L. V. Bravina, and D. H. Rischke. Antiflow of nucleons at the softest point of the EoS. *Phys. Rev.*, C61:024909, 2000.

[23] Horst Stoecker. Collective flow signals the quark gluon plasma. *Nucl. Phys.*, A750:121–147, 2005.

[24] L. Adamczyk et al. Beam-Energy Dependence of the Directed Flow of Protons, Antiprotons, and Pions in Au+Au Collisions. *Phys. Rev. Lett.*, 112(16):162301, 2014.

[25] A. Adare et al. Beam-energy and system-size dependence of the space-time extent of the pion emission source produced in heavy ion collisions. 2014.

[26] Roy A. Lacey. Indications for a Critical End Point in the Phase Diagram for Hot and Dense Nuclear Matter. *Phys. Rev. Lett.*, 114(14):142301, 2015.

[27] Misha A. Stephanov, K. Rajagopal, and Edward V. Shuryak. Event-by-event fluctuations in heavy ion collisions and the QCD critical point. *Phys. Rev.*, D60:114028, 1999.

[28] J. T. Mitchell. The RHIC Beam Energy Scan Program: Results from the PHENIX Experiment. *PoS*, CPOD2013:003, 2013.

[29] L. Adamczyk et al. Beam energy dependence of moments of the net-charge multiplicity distributions in Au+Au collisions at RHIC. *Phys. Rev. Lett.*, 113:092301, 2014.

[30] J. B. Elliott et al. The Liquid to vapor phase transition in excited nuclei. *Phys. Rev. Lett.*, 88:042701, 2002.

[31] Roy A. Lacey, Peifeng Liu, Niseem Magdy, B. Schweid, and N. N. Ajitanand. Finite-Size Scaling of Non-Gaussian Fluctuations Near the QCD Critical Point. 2016.